Synthesis of Indolostilbenes via FeCl$_3$-promoted Oxidative Cyclisation and their Biological Effects on NG108-15 Cell Viability and H$_2$O$_2$-induced Cytotoxicity

Mohamad Nurul Azmi,[1*] Tan Aik Sian,[1] Munirah Suhaimi,[2] Muhamad Noor Alfarizal Kamarudin,[3] Mohd Fadzli Md Din,[1] Mohd Azlan Nafiah,[4] Noel F. Thomas,[5] Habsah Abdul Kadir[6] and Khalijah Awang[2]

[1]School of Chemical Sciences, Universiti Sains Malaysia,
11800 USM Pulau Pinang, Malaysia
[2]Department of Chemistry, Faculty of Science, University of Malaya,
50603 Kuala Lumpur, Malaysia
[3]Brain Research Institute, Jeffrey Cheah School of Medicine and Health Sciences,
Monash University Malaysia, Jalan Lagoon Selatan,
47500 Bandar Sunway, Selangor, Malaysia
[4]Department of Chemistry, Faculty of Science and Mathematics,
Sultan Azlan Shah Campus, Universiti Pendidikan Sultan Idris,
Proton City, 35950 Behrang, Perak, Malaysia
[5]Methodist College Kuala Lumpur, Kuala Lumpur, Malaysia
[6]Biomolecular Research Group, Biochemistry Program, Institute of Biological Sciences,
Faculty of Science, University of Malaya, 50603 Kuala Lumpur, Malaysia

*Corresponding author: mnazmi@usm.my

ABSTRACT: *A convenient and simple radical cation cyclisation of 3,5-dimethoxystilbene was developed using the commercially available FeCl$_3$ under mild condition. It enabled the construction of a new class of indolostilbenes (i.e., indole-stilbene hybrid). Various parameters were investigated to obtain better yields (more than 42%) compared with the previously reported. The synthesised indolostilbenes were characterised, and their mechanism of formation was discussed. The synthesised compounds were submitted for biological assay on NG108-15 cell viability and H$_2$O$_2$-induced cytotoxicity. The result showed that two indolostilbenes have promising protective activity against H$_2$O$_2$.*

Keywords: Indolostilbene, FeCl$_3$ oxidative coupling, pericyclic reaction, H$_2$O$_2$ protective properties, cyclisation

1.   INTRODUCTION

Neurodegenerative diseases such as dementia (Parkinson's, Huntington's and Alzheimer's diseases) and stroke result in significant disabilities and dependency among the elders worldwide.[1] The progression of these neurodegenerative diseases is attributed to various factors. For instance, these diseases can be initiated by oxidative stress-induced cell damage corresponding to the overproduction of reactive oxygen species (ROS) such as hydrogen peroxide (H_2O_2). H_2O_2 acts as the precursor of ROS, which, in excess, induces oxidative stress that leads to neuronal cell apoptosis.[2,3] The overproduction of ROS promotes mitochondrial dysfunction leading to protein, lipid and DNA damage.[2,3] Based on these observations, it may be beneficial to study the capability of newer therapeutic agents in mitigating H_2O_2-induced apoptosis in the treatment of neurodegenerative diseases.[2,3] Therefore, chemists have been actively synthesising new classes of active compounds that possess H_2O_2 protective properties to combat neurodegenerative diseases.

Stilbenes are the family of bioactive compounds found in plants.[4] *Trans*-resveratrol, *o*-carboxamido stilbene, piceid, piceatannol, astringin, pterostilbene and oligomers (viniferin and hopeaphenol) are the groups of compounds from this family (Figure 1).[4] Stilbenes have received considerable attention because of their potent health-promoting properties, such as preventing cancers, cardiovascular and neurodegenerative diseases.[5–13] Oligostilbenes such as pallidol, balanocarpol and (+)-*α*-viniferin also show a variety of biological activities (Figure 1).[14–17]

Indoles have gained much attention from medical and synthetic chemists due to its ability to act as a free radical scavenger and antioxidant property. This resulted in the synthesis of a new class of oligostilbenes, namely, indolostilbene.[18] Indolostilbene is the polymeric form of stilbene that has the indole ring.[19] Previous study has shown that the indole ring in the molecule is the reactive site for oxidation. This is due to its highly stable resonance and relatively low activation energy gap for free radical reactions.[20,21] Thus, in this paper, we discussed the synthesis of a new group of indolostilbenes and their protective activity against H_2O_2-induced cell death in NG108-15 cells. To our knowledge, this is the first report on optimising and synthesising these new indolostilbenes and their biological activity.
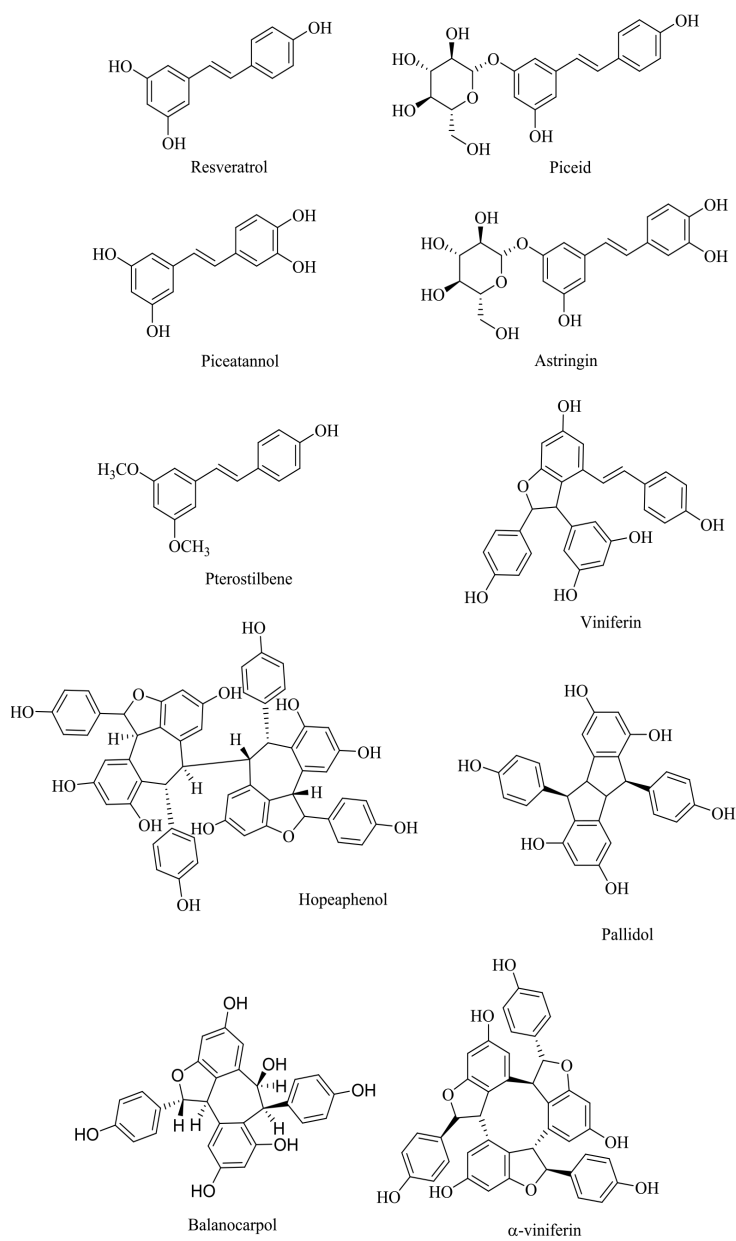
Figure 1: Examples of stilbenes and oligostilbenes.

2.   EXPERIMENTAL

2.1   General

Unless otherwise noted, materials were purchased from Sigma-Aldrich Co., Acros Organics and Merck Chemical Co., and used without purification. Dimethylformamide (DMF) was dried over 4Å molecular sieves (Merck) before use. Column chromatography was carried out using silica gel from Merck (40–63 µm). For thin-layer chromatography, Merck TLC aluminium sheets (silica gel 60 F_{254}) were used. All reactions were carried out in heat-dried glassware under a dry nitrogen atmosphere unless otherwise stated. All liquid transfer was conducted using standard syringe or cannula techniques. All spectral data were obtained on the following instruments: infrared spectra were recorded on a Perkin Elmer FTIR Spectrum RX-1 spectrometer at wavenumber from 4000–400 cm^{-1}. Nuclear magnetic resonance spectra were obtained on a Bruker AVN 500 MHz spectrometer from Bruker Bioscience, Billerica, MA, United States) and the spectra were reported in ppm units on the δ scale, relative to $CDCl_3$. The proton, ^{1}H resonance was recorded at 500 MHz and ^{13}C at 125 MHz. The coupling constants are given in Hz. The mass spectra were measured using Agilent 6530 Accurate-Mass QTOF LC/MS system. The HPLC analysis was done using Waters auto purification system (Waters 2767 and 2996).

2.2   Materials

The NG108-15 hybridoma cell line (ATCC® HB-12317™) was obtained from American Type Culture Collection (ATCC). Dulbecco's Modified Eagle's Medium (DMEM), epigallocatechin gallate (EGCG), Hypoxanthine-Aminopterin-Thymidine (HAT), phosphate-buffered saline (PBS), sodium bicarbonate, HEPES salt and 3-(4,5-dimethylthiazol-2-yl)-2,5-diphenyltetrazolium bromide (MTT) were obtained from Sigma-Aldrich. Foetal bovine serum (FBS) (100 unit ml^{-1}), penicillin (100 µg ml^{-1}), streptomycin and amphotericin B (50 µg ml^{-1}) were supplied by PAA Laboratories. Accutase was bought from Innovative Cell Technologies, Inc. Hydrogen peroxide (H_2O_2) was purchased from Systerm®. All chemicals used were of analytical and molecular grade.

2.3   Procedure for the Preparation of Compounds

2.3.1   Procedure for synthesis of styrene 2, protected amide 4 and stilbene 5

The procedure for the preparation of styrene **2**, protected amide **4** and stilbene **5** was reported previously by our group.[6] The detailed procedure and spectroscopic data are attached in the supplementary information.

2.3.2   Procedure for indolostilbenes 8 and 9

3,5-Dimethoxystilbene **5** (0.25 g, 0.9 mmol) was dissolved in 50.0 ml dichloromethane. Anhydrous $FeCl_3$ (0.69 g, 4.2 mmol) was then added to the mixture under nitrogen. The mixture was stirred for 7 h at room temperature and monitored by TLC. After consuming the starting material, the reaction mixture was diluted with aqueous ammonium chloride solution and extracted with ethyl acetate (3×25.0 ml). The combined ethyl acetate extracts were dried over anhydrous sodium sulphate. The crude product was finally purified by column chromatography (using the solvent system: hexane/ethyl acetate; $80:20 \rightarrow 70:30$) which afforded *ortho*-acetamidobenzaldehyde **6** and dichlorostilbene **7**, and two dimers **8** and **9**, in 6% (1.9 mg), 10% (7.5 mg), 43% (56.7 mg) and 42% (55.7 mg) yields, respectively. The spectroscopic data are compared with our previous data.[19]

2.4   HPLC Analysis of Crude Reaction

The HPLC analysis was done using Waters auto purification system equipped with a sample manager (Waters 2767), a binary pump, an automatic injector and a photodiode array detector (190–600 nm, Waters 2996). The separation was carried out on a Waters® X-Bridge C18 column (250×4.6 mm, 5.0 μm). An isocratic solvent system of 25% H_2O: 75% acetonitrile was used with the flow rate of 1.0 ml min^{-1}.

2.5   Cell Culture

The NG108-15 cells were cultured in DMEM supplemented with 10% heat-inactivated FBS, 2% penicillin/streptomycin, 1% amphotericin B and HAT as a complete medium. The cells were cultured at 37°C in 5% CO_2 atmosphere with 95% humidity and checked routinely under an inverted microscope (Motic) for any contamination.

2.6   Assessment of Biological Activity

The biological activity of indolostilbenes was evaluated in NG108-15 by using MTT cell viability assay.[22] Metabolically active cells containing mitochondrial dehydrogenase converted the tetrazolium salt and MTT into insoluble purple formazan crystals at a rate proportional to the cell viability. The NG108-15 cells were rinsed with PBS, harvested with accutase, plated at a total density of 5.0×10^3 cells/well in a 96-well plate and left to adhere for 24 h. Cells were preincubated for 2 h with indolostilbenes **8** and **9** (3.125–100 µM) before H_2O_2 (400 µM) exposure for subsequent 24 h. EGCG (1–50 µM) was used as a positive control. A 20 µl MTT solution (5 mg ml^{-1}) was added and incubated at 37°C for another 4 h. The medium was removed, and DMSO was added to dissolve the formazan crystals. The absorbance reading was measured directly using a microplate reader (ASYS UVM340) at 570 nm (with a reference wavelength of 650 nm). Cell viability was calculated based on the formula below:

$$\% \text{ of cell viability} = \text{ absorbance of treated cells (As)/ absorbance of control cells (AC)} \times 100 \%$$

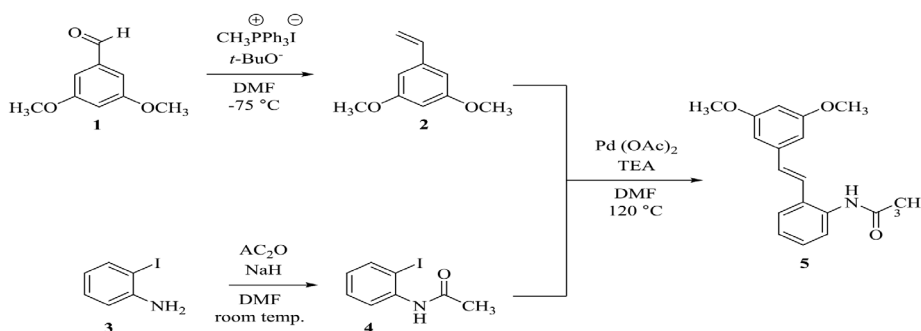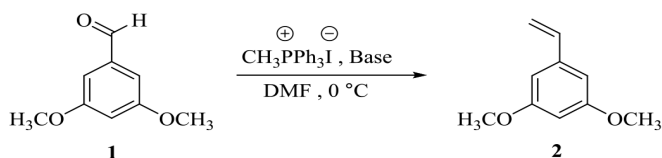## 2.7   Statistical Analysis

The biological assays were conducted in triplicate, and the data was presented in means ± standard error (SE). Student's t-test and Mann's Whitney were used to determining the statistical significance (p values < 0.05) and differences between the control, untreated and treated groups were discussed. Statistical analyses between treated groups were determined using one-way ANOVA and Dunnett's test (significant $^\#p$ values < 0.05).

3.   RESULTS AND DISCUSSIONS

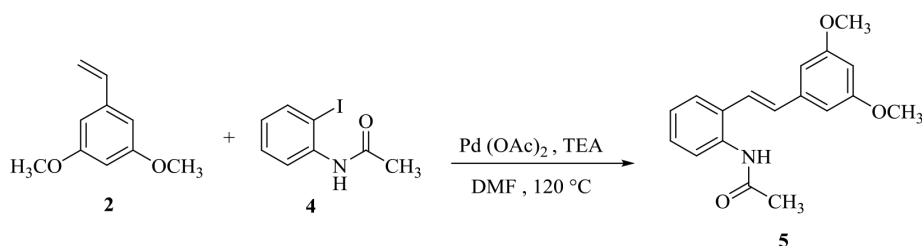## 3.1   Synthesis of Indolostilbenes 9 and 10

Initially, the building blocks were synthesised under an optimised condition with various catalyst, time and reaction conditions (Tables 1 and 2). The styrene **2** was obtained via our optimised Wittig reaction in 91% yield from the corresponding aldehyde **1** (Scheme 1) as shown in Table 1.

Scheme 1: The synthesis of 3,5-dimethoxystilbene **5.**

Table 1:   The experimental condition and yield for the synthesis of 3,5-dimethoxystyrene **2** via Wittig reaction.

Entry	Base (mol equiv.)	Solvent	Yield[a] (%)
1[b]	NaH (5)	DMF[c]	43
2	NaH (5)	DMF[d]	7
3	NaH (3)	DMF[d]	16
4	NaH (7)	DMF[d]	41
5	t-BuO⁻ (1)	DMF[c]	1
6	t-BuO⁻ (1)	DMF[d]	91

Notes: [a]Isolated yields after column chromatography; [b]data from the previous report; [c]the reactions were carried out in dry solvent and under nitrogen gas for 24 h; [d]the reactions were carried out in non-dry solvent and under nitrogen gas for 24 h.
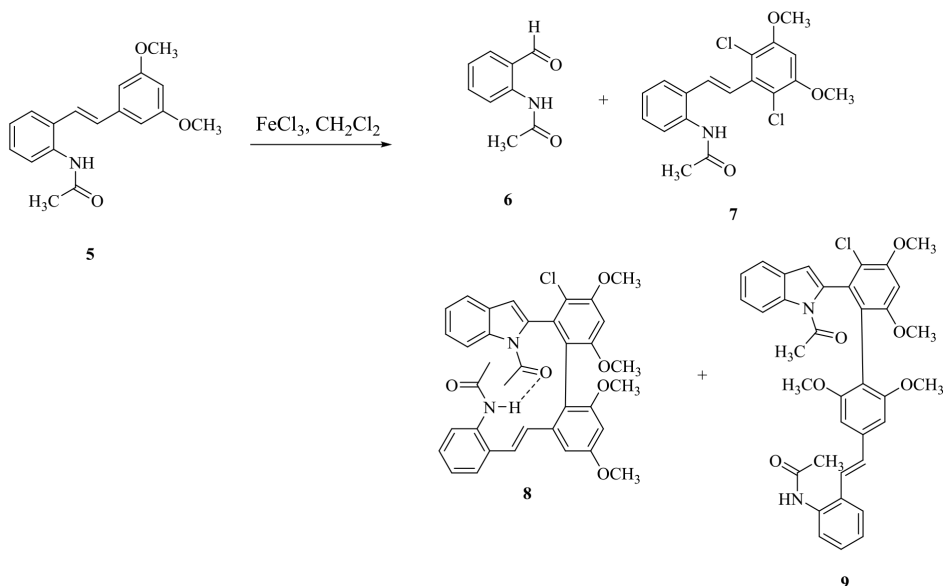
The Heck coupling proceeded smoothly according to our protocol, as shown in Table 2 and Scheme 1. The Heck reaction was performed by heating at 120°C to the corresponding styrene **2** with acetamide **4** in the presence of Pd(OAc)$_2$ in dry DMF for 24 h. The corresponding stilbene **5** was generated in yields exceeding 76% (Table 2).

Table 2:   The experimental condition and yield for the synthesis of 3,5-dimethoxystilbene **5.**

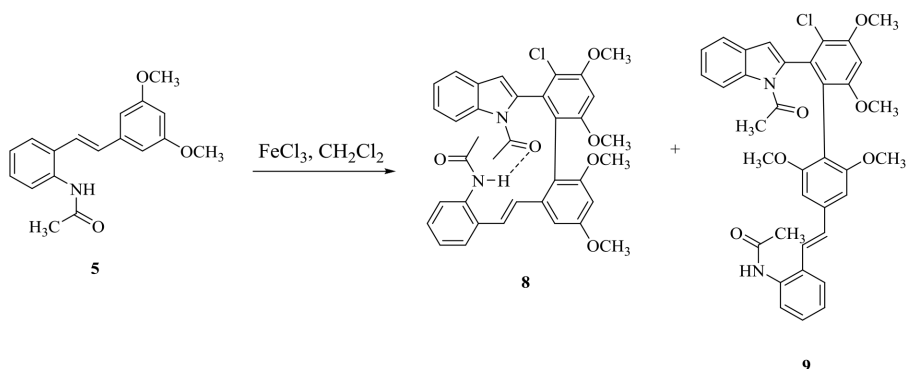| Entry	$Pd(OAc)_2$ (mol equiv.)	TEA (mol equiv.)	Solvent	Time (hours)	Yield[a] (%)
1[b]	1/65	1/34	DMF	48	45
2	1/45	3	DMF	48	30
3	0.01	3	DMF	48	50
4	0.01	3	DMF	30	69
5	0.01	3	DMF	24	76

Notes: [a]Isolated yields after column chromatography; [b]data from the previous report

The 3,5-dimethoxystilbene **5** was subjected to anhydrous $FeCl_3$ oxidation (1:5 molar ratio, Scheme 2). Four products were isolated, i.e., an *ortho*-acetamidobenzaldehyde **6,** dichlorostilbene **7** and two dimers **8** and **9**. Compounds **8** and **9** contained an intact stilbene olefinic bond (Scheme 2). *Ortho*-acetamidobenzaldehyde **6** was identified by the presence of an aldehyde peak at δ_H 9.90 and δ_C 195.7 (in the ^1H and ^{13}C NMR, respectively) resulting from cleavage of the stilbene double bond. Apart from the mass spectrometric evidence for incorporating two chlorines into the molecule, the ^{13}C chemical shift for C-2 and C-6 of dichlorostilbene **7** was observed at δ_C 114.0. The HRESIMS of dimers **8** and **9** showed a pseudo-molecular ion peak at *m/z* 648 and *m/z* 625, respectively, corresponding to the molecular formula of $C_{36}H_{33}ClN_2NaO_6$ (*m/z* 648.1998 ([M + Na]$^+$; calcd. 648.1998) and $C_{36}H_{34}ClN_2O_6$ (*m/z* 625.2111 ([M + H]$^+$; calcd. 625.2105). These data indicate the incorporation of one chlorine atom in both **8** and **9**.

Scheme 2: The oxidative coupling of 3,5-dimethoxystilbene **5**.

Previously, Kartini et al. isolated these indolostilbenes **8** and **9** at a low yield, i.e., 14% and 10%, respectively.[19] To obtain further insights into the oxidative cyclisation, control experiments (the solvent volume, the temperature of reaction and the proportion of Lewis acid) were examined using $FeCl_3$ as the catalyst (Table 3). From these reactions and careful examination of the variety of reaction condition, 5.0 equiv. of $FeCl_3$ in 50 ml dichloromethane at room temperature leads to a drastic improvement in yield of the indolostilbenes **8** and **9** at 43% and 42%, respectively. Trace amounts of *ortho*-acetamidobenzaldehyde **6** and dichlorostilbene **7** were also detected. Use of low temperature did not result in the formation of the indolostilbenes, while high temperatures resulted in low product yield. The use of dilute concentration of reactants improved the yield of the product in the radical cation reaction.[19,23,24] In this radical reaction, the optimum ratio between stilbene and the oxidant is 1:5. Further increase in the oxidant will drastically decrease the target molecules, resulting in the stilbene decomposition. Dichloromethane was found to be an excellent solvent for this reaction, aiding in the electrophilic chlorination step in the formation of chlorophenylindole **15**, which was an intermediate in the formation of indolostilbenes **8** and **9** (Scheme 3). The use of acetone as the solvent did not result in the formation of indolostilbenes **8** and **9** (Table 3).

Table 3:   The experimental conditions and yield during the FeCl$_3$ oxidative coupling of 3,5-dimethoxystilbene **5.**

Entry	Conditions	Time (h)	Yield[a] (%)	
			8	**9**
1[b]	FeCl$_3$ (5.0 equiv), DCM (10 ml), rt	7	14	10
2	FeCl$_3$ (5.0 equiv), DCM (10 ml), rt	7	7	6
3	FeCl$_3$ (5.0 equiv), DCM (50 ml), rt	7	43	42
4	FeCl$_3$ (7.0 equiv), DCM (50 ml), rt	7	14	14
5	FeCl$_3$ (10.0 equiv), DCM (50 ml), rt	7	12	12
6	FeCl$_3$ (5.0 equiv), DCM (50 ml), 0–4°C	7	–	–
7	FeCl$_3$ (5.0 equiv), DCM (50 ml), 40–50°C	7	32	31
8	FeCl$_3$ (5.0 equiv), Acetone (50 ml), rt	7	–	–
9	FeCl$_3$ (5.0 equiv), ACN (50 ml), rt	7	–	–

Notes: [a]Isolated yields after column chromatography; [b]data from the previous publication.

3.2   HPLC Analysis

The crude extract of FeCl$_3$ oxidative cyclisation was injected into an HPLC system. The chromatogram (Figure 2) was recorded at 254 nm. Dichlorostilbene **7**, indolostilbene **8** and **9** gave the sharp peaks at t_R = 13.7 min, 26.5 min and 34.57 min, respectively.
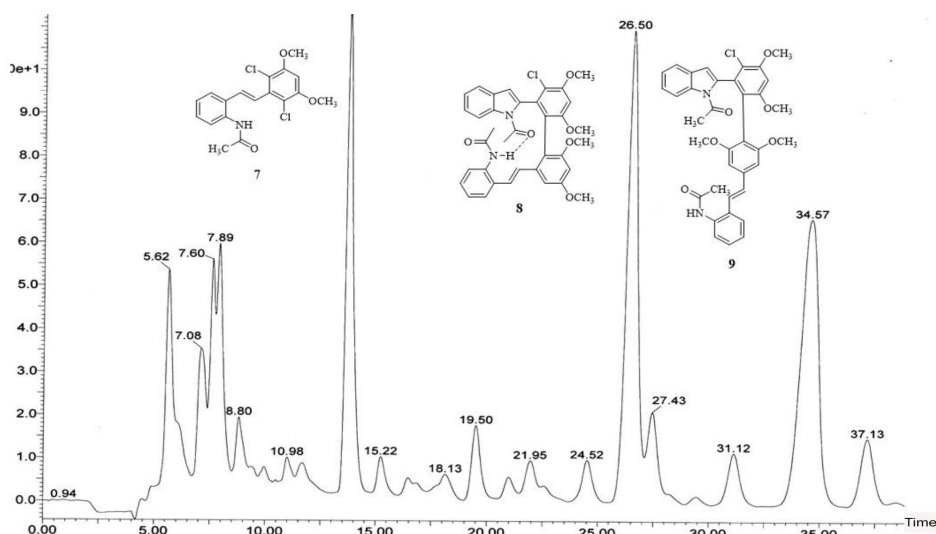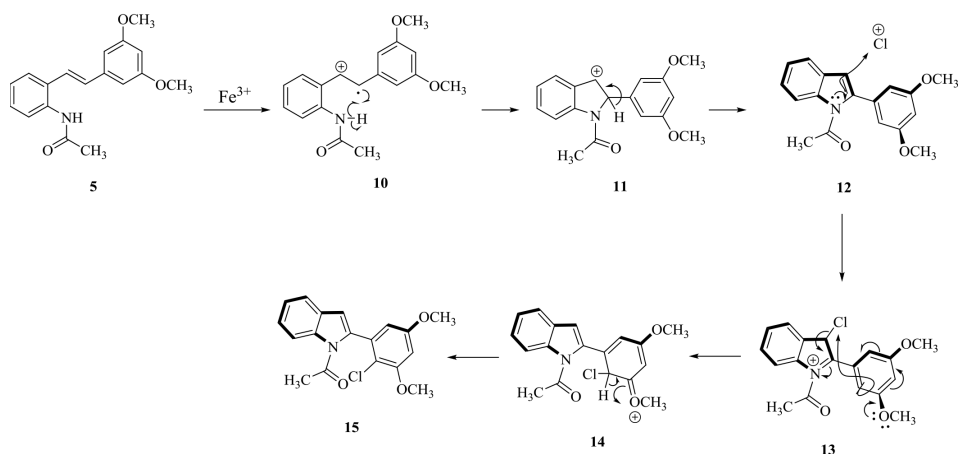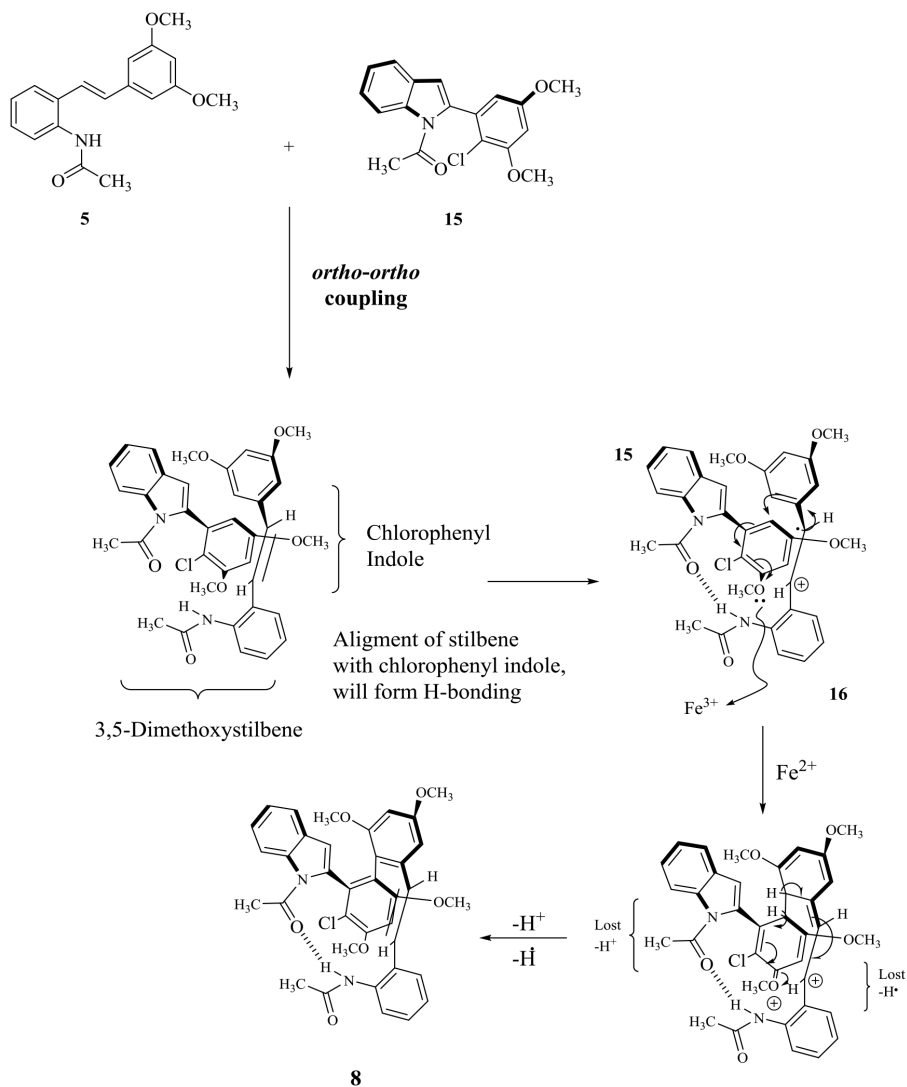
Figure 2: The HPLC chromatogram of the crude FeCl$_3$ oxidative cyclisation products.
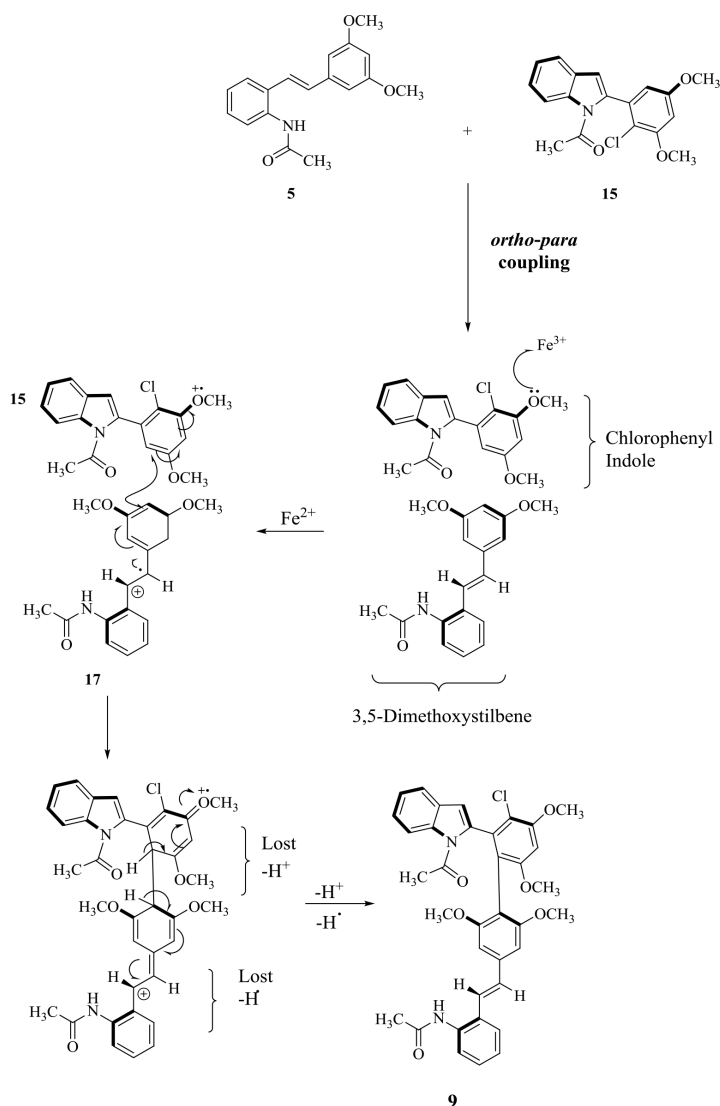
3.3   Mechanism Study

The 3,5-dimethoxystilbene has produced aldehyde **6**, dichlorostilbene **7**, and the unprecedented indolostilbene dimers **8** and **9**. The formation of all target compounds was already described in our previous publication.[19] For the formation of indolostilbenes **8** and **9**, the oxidation of 3,5-dimethoxystilbene **5** generates the radical cation **10**. This proceeds with the formation of indole **12** by the rapid deprotonation of **11**. Electrophilic chlorination of **12** via indolenium species **13** will give chlorophenylindole **15** (Scheme 3).

Scheme 3: The mechanism for the formation of chlorophenylindole **15**.

In Scheme 4, the alignment of stilbene **5** and chlorophenylindole **15** will give rise to two indolostilbenes **8** and **9**. The oxidation of the olefinic bond in **5** produces the radical cation **16**, which attacks the chlorophenylindole **15**. The removal of an electron from the phenyl ring sets up the *ortho-ortho* oxidative coupling, forming the stereogenic axis between ring B and D for compound **8**. Besides, the *ortho-para* coupling of both radical cation **17** and chlorophenyl indole **15**, sets up the formation of compound **9** (Schemes 4 and 5).

Scheme 4: The oxidative cyclisation of chlorophenyl indole **15** and stilbene **5** leading to indolostilbene **8** via the *ortho-ortho* coupling.

Scheme 5: The oxidative cyclisation of chlorophenyl indole **15** and stilbene **5** leading to
indolostilbene **9** via *ortho-para* coupling.

3.4 Protectivity of Indolostilbene Against H_2O_2-induced Cytotoxicity

The concentration-dependence of H_2O_2 that reduced the NG108-15 cell viability
was first optimised. The concentration selected was 400 μM as the cell viability
of H_2O_2-treated cell at this concentration was decreased to $50 \pm 1\%$ after 24 h

exposure, as summarised in Table 4 and Figure 3(a-b). The concentration of H_2O_2 was optimised in our previous study using H_2O_2 concentration ranging from 0.1–2 mM at 24 h.[25] Based on the optimisation, 400 µM of H_2O_2 significantly reduced the NG108-15 cell viability around 50%. Thus, this concentration was selected for the protective evaluation. Prior to the pretreatment with indolostilbenes, the NG108-15 was treated with H_2O_2 at various concentration, similar to our previous study. It was reported that at 400 µM, H_2O_2 reduced the NG108-15 cell viability to 50% compared to untreated control cells. Thus, this concentration was selected for the H_2O_2 protective evaluation in the MTT assay. The pre-treatment with indolostilbene **8** at 100 µM significantly increased the cell viability to 72±1% as compared to H_2O_2-treated cells (Figure 3(a)). Meanwhile, pre-treatment with indolostilbene **9** at 50 µM (Figure 3(b)) significantly increased the cell viability to 80±1%.

Interestingly, indolostilbene **9** pre-treatment at 100 µM resulted in a lower protection value compared at 50 µM. This suggests the possibility of indolostilbene **9** exhibiting toxicity at a higher dose. Due to indolostilbene **9** toxicity effects, H_2O_2 protective effect of indolostilbene **8** was more dose-dependent than indolostilbene **9**. Even though both indolostilbene **8** and **9** showed lower H_2O_2 protective activity when compared to EGCG (Table 4), it was significantly different ($^*P < 0.05$) compared to the H_2O_2-treated group.

From the structure-activity relationship (SAR), we can conclude that both compounds contain an indole and stilbene cores, 3,5-dimethoxy B ring and N-acetamide substituent. However, the coupling position between an indole and stilbene moieties may cause differences in the activity. For compound **9** which is coupling at *ortho-para* position show a good activity at 80±1% for NG108-15 cell viability at the minimal concentration (50 µM) compared to compound **8** which is coupling at *ortho-ortho* position (72±1% cell viability at 100 µM). Interestingly, the formation of intramolecular hydrogen bonding in compound **8** between N-H amide in stilbene moiety and C=O amide in the indole moiety, make the compound well packed, rigid and decrease the activity. Meanwhile, the intramolecular H-bonding for compound **9** is impossible, and the compound is free to rotate. This evidence has been supported by PM6/MOPAC2007 calculation in our previous publication.[19]
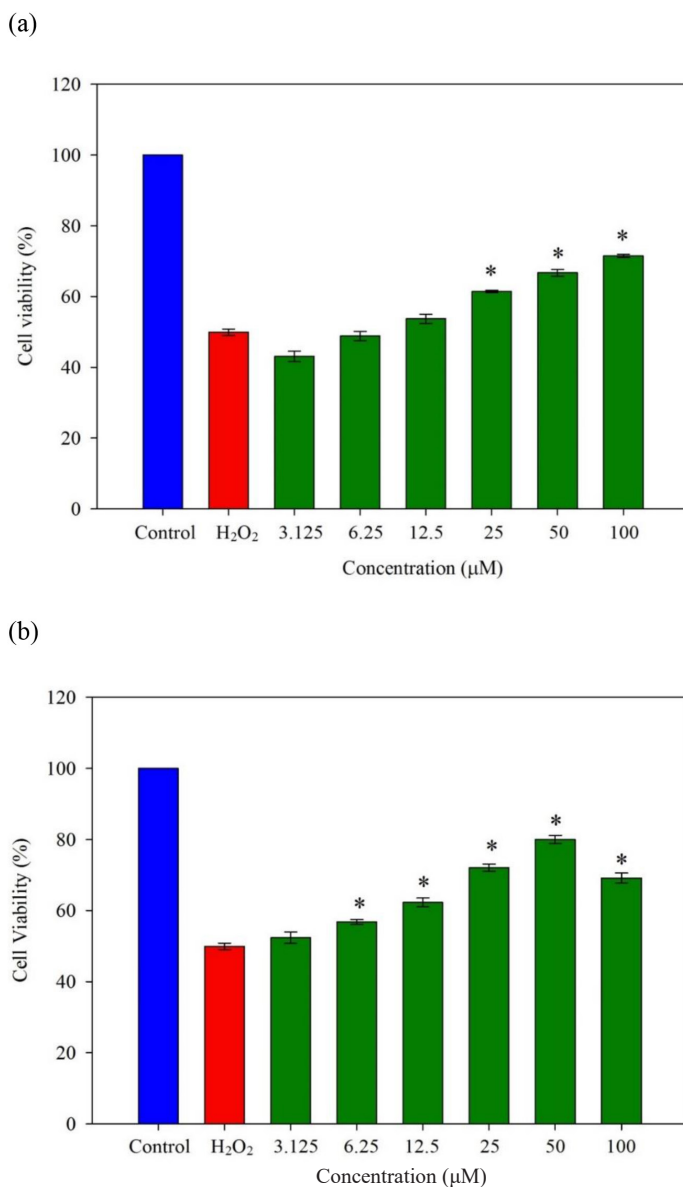
(a)

(b)

Figure 3: Illustrations of (a) biological activity of indolostilbene **8** against H_2O_2-induced cell death by MTT cell viability assay; (b) increment in cell viability by pre-treatment with indolostilbene **9** in H_2O_2-induced cell death prior to exposing it to 400 μM H_2O_2 for 24 h. Values are taken at mean ± S.E. from at least three independent experiments. The asterisk indicated significantly different values from H_2O_2-treated cells ($^*P < 0.05$).

Table 4: The biological activity of indolostilbenes **8** and **9** against H_2O_2-induced apoptosis in NG108-15 cells.

Compound	Concentration (μM)	Cell Viability (%)[b]
Control	–	100
H_2O_2[c]	400	50 ± 1[#]
8	100	72 ± 1[*]
9	50	80 ± 1[*]
EGCG (50 μM)[d]	–	85 ± 2[*]

Notes: The values shown are the means ± SE of at least three independent experiments.
[a] NG108-15 cells were pre-treated with compounds (3.125–100 μM) for 2 h prior to exposure to H_2O_2 (400 μM). After incubation, cells were assessed by MTT to determine the percentage viability.
[b] Cell viability was measured by MTT assay.
[c] H_2O_2-treated value differed significantly from the untreated control at the level of [#]$P < 0.05$.
[d] EGCG was used as the standard positive control.
[#] Results differ significantly from the H_2O_2-treated group compared to the untreated control group: $P < 0.05$.
[*] Significantly from H_2O_2-treated group compared to the treatment group: $P < 0.05$

NG108-15 is a somatic cell hybrid of glioma of rat (*Rattus norvegicus*) and neuroblastoma of mouse (*Mus musculus*), which was developed in 1971 by Hamprecht by the fusion of mouse N18TG2 neuroblastoma cells with rat C6-BU-1 glioma cells in the presence of inactivated Sendai virus.[26,27] The NG108-15 cell line is a suitable choice because it exhibits angiotensin II receptor. It can be further differentiated into a cholinergic phenotype cell line with voltage-dependent membrane currents, acetylcholine release and the formation of cholinergic synapses.[28–30] Furthermore, NG108-15 has been extensively used as the in-vitro neuroprotective neuronal model using various phytochemicals[25,31,32] and neuritogenesis studies.[33–36] Considering its previous use, NG108-15 is a suitable neuronal model for the in vitro neuroprotective study reported herein.

4.   CONCLUSION

In summary, we have developed a simple and efficient method to synthesise indolostilbene via ferric chloride oxidative cyclisation. The synthesised stilbenes were evaluated for H_2O_2 protective activity. The optimum condition was achieved by using 5.0 equiv. of anhydrous $FeCl_3$ in dichloromethane as the solvent. It gives an excellent yield of up to 43% and 42% of indolostilbenes **8** and **9**, respectively. It was observed that the dichloromethane was involved in the formation of chlorophenylindole **15** as an intermediate for the formation of indolostilbene **8** and **9**. In addition, the indolostilbenes **8** and **9** showed potent protective activity against H_2O_2 in NG108-15 cells. Pretreatment with both compounds significantly

increased the NG108-15 cell viability to 70%±1% (at 100 μM) and 80%±1% (at 50 μM) respectively. These were significantly different ($^*P < 0.05$) compared to the H_2O_2-treated group (50%±1%). Although the H_2O_2 protective effects of indolostilbenes **8** and **9** were not as potent as EGCG, their protective effect against H_2O_2 was significantly higher than the H_2O_2-treated value, with an increase in cell viability between 21%–31%. However, further studies are needed to understand the mechanism of action involved in the H_2O_2-induced intracellular pathway leading to cell apoptosis.

5.   ACKNOWLEDGEMENTS

6.   REFERENCES

1.   Feigin, V. et al. (2019). Global, regional, and national burden of neurological disorders, 1990–2016: A systematic analysis for the Global Burden of Disease Study 2016. *Lancet Neurol.*, 18(5), 459–480. https://doi.org/10.1016/S1474-4422(18)30499-X

2.   Liu, Z. et al. (2017). Oxidative stress in neurodegenerative diseases: From molecular mechanisms to clinical applications. *Oxid. Med. Cell. Long*., Article ID 2525967. https://doi.org/10.1155/2017/2525967

3.   Elfawy, H. A. & Das, B. (2019). Crosstalk between mitochondrial dysfunction, oxidative stress, and age-related neurodegenerative disease: Etiologies and therapeutic strategies. *Life Sci.*, 218, 165–184. https://doi.org/10.1016/j.lfs.2018.12.029

4.   Chong, J., Poutaraud, A. & Hugueney, P. (2009). Metabolism and roles of stilbenes in plants. *Plant Sci.*, 177(3), 143–155. https://doi.org/10.1016/j.plantsci.2009.05.012

5.   Tellone, E. et al. (2019). Resveratrol. In (Eds.) Nabavi, S. M. & Silva, A. S., *Nonvitamin and nonmineral nutritional supplements.* New York: Academic Press, 107–110. https://doi.org/10.1016/B978-0-12-812491-8.00014-X

6.   Azmi, M. N. et al. (2013). Design, synthesis, and cytotoxic evaluation of *o*-carboxamido stilbene analogues. *Int. J. Mol. Sci.*, 14(12), 23369–23389. https://doi.org/10.3390/ijms141223369

7.   Romero-Pérez, A. I. et al. (1999). Piceid, the major resveratrol derivative in grape juices. *J. Agric. Food Chem.*, 47(4), 1533–1536. https://doi.org/10.1021/jf981024g

8.   Seyed, M. A. et al. (2016). A comprehensive review on the chemotherapeutic potential of piceatannol for cancer treatment, with mechanistic insights. *J. Agric. Food Chem.*, 64(4), 725–737. https://doi.org/10.1021/acs.jafc.5b05993

9.   Fauconneau, B. et al. (1997). Comparative study of radical scavenger and antioxidant properties of phenolic compounds from *Vitis vinifera* cell cultures using in vitro tests. *Life Sci.*, 61(21), 2103–2110. https://doi.org/10.1016/S0024-3205(97)00883-7

10.   Chang, J. et al. (2012). Low dose pterostilbene, but not resveratrol, is a potent neuromodulator in aging and Alzheimer's disease. *Neurobiol. Aging*, 33(9), 2062–2071. https://doi.org/10.1016/j.neurobiolaging.2011.08.015

11.   McCormack, D. & McFadden, D. (2012). Pterostilbene and cancer: Current review. *J. Surg. Res.*, 173(2), e53–e61. https://doi.org/10.1016/j.jss.2011.09.054

12.   Zghonda, N. et al. (2012). ε-Viniferin is more effective than its monomer resveratrol in improving the functions of vascular endothelial cells and the heart. *Biosci., Biotechnol., Biochem.*, 76(5), 954–960. https://doi.org/10.1271/bbb.110975

13.   Empl, M. T. et al. (2014). The growth of the canine glioblastoma cell line D-GBM and the canine histiocytic sarcoma cell line DH82 is inhibited by the resveratrol oligomers hopeaphenol and r2-viniferin. *Vet. Comp. Oncol.*, 12(2), 149–159. https://doi.org/10.1111/j.1476-5829.2012.00349.x

14.   Matsuura, B. S. et al. (2015). A scalable biomimetic synthesis of resveratrol dimers and systematic evaluation of their antioxidant activities. *Angew. Chem., Int. Ed.*, 127(12), 3825–3828. https://doi.org/10.1002/anie.201409773

15.   Mora-Pale, M. et al. (2015). Antimicrobial mechanism of resveratrol-*trans*-dihydrodimer produced from peroxidase-catalysed oxidation of resveratrol. *Biotechnol. Bioeng.*, 112(12), 2417–2428. https://doi.org/10.1002/bit.25686

16.   Atun, S. et al. (2008). Resveratrol derivatives from stem bark of *Hopea* and their biological activity test. *J. Phys. Sci.*, 19(2), 7–21.

17.   Dilshara, M. G. et al. (2014). Anti-inflammatory mechanism of *α*-viniferin regulates lipopolysaccharide-induced release of proinflammatory mediators in BV2 microglial cells. *Cell. Immunol.*, 290(1), 21–29. https://doi.org/10.1016/j.cellimm.2014.04.009

18.   Shirinzadeh, H. et al. (2016). Novel indole-based melatonin analogues substituted with triazole, thiadiazole and carbothioamides: Studies on their antioxidant, chemopreventive and cytotoxic activities. *J. Enz. Inhib. Med. Chem.*, 31(6), 1312–1321. https://doi.org/10.3109/14756366.2015.1132209

19.   Ahmad, K. et al. (2009). A FeCl$_3$-promoted highly atropodiastereoselective cascade reaction: synthetic utility of radical cations in indolostilbene construction. *Tetrahed.,* 65(7), 1504–1516. https://doi.org/10.1016/j.tet.2008.11.100

20.   Tan, D. et al. (2005). Chemical and physical properties and potential mechanisms: melatonin as a broad-spectrum antioxidant and free radical scavenger. *Curr. Top. Med. Chem.*, 2(2), 181–197. https://doi.org/10.2174/1568026023394443

21.   Bozkayaa, P. et al. (2006). Determination and investigation of electrochemical behavior of 2-phenylindole derivatives: discussion on possible mechanistic pathways. *Can. J. Anal. Sci. Spectrosc.*, 51(3), 125–139. https://doi.org/20.500.12575/70709

22.   Mosmann, T. (1983). Rapid colorimetric assay for cellular growth and survival: Application to proliferation and cytotoxicity assays. *J. Immunol. Meth*, 65(1–2), 55–63. https://doi.org/10.1016/0022-1759(83)90303-4

23. Thomas, N. F. et al. (2008). The subtle co-catalytic intervention of benzophenone in radical cation mediated cyclisation - An improved synthesis of 2-(3', 4'-dimethoxyphenyl)indoline. *Heteroc.*, 75(5), 1097–1108. https://doi.org/10.3987/COM-07-11280

24. Kee, C. H. et al. (2011). Cyclisation vs. cyclisation/dimerisation in *o*-amidostilbene radical cation cascade reactions: the amide question. *Mol.*, 16(9), 7267–7287. https://doi.org/10.3390/molecules16097267

25. Kamarudin, M. N. A. et al. (2014). (*R*)-(+)-α-lipoic acid protected NG108-15 cells against H_2O_2-induced cell death through PI3K-Akt/GSK-3β pathway and suppression of NF-κβ-cytokines. *Drug Des., Dev. Ther.*, 8, 1765–1780. https://doi.org/10.2147/DDDT.S67980

26. Hamprecht, B. et al. (1985). *Methods in enzymology.* London: Academic Press. https://doi.org/10.1016/0076-6879(85)09096-6

27. Wong, K. H. et al. (2007). Activity of aqueous extracts of lion's mane mushroom *Hericium erinaceus* (Bull.: Fr.) Pers. (Aphyllophoromycetideae) on the neural cell line NG108-15. *Int. J. Med. Mush.*, 9(1), 57–65. https://doi.org/10.1615/IntJMedMushr.v9.i1.70

28. Kasai, H. (1992). Voltage-and time-dependent inhibition of neuronal calcium channels by a GTP-binding protein in a mammalian cell line. *J. Physiol.*, 448(1), 189–209. https://doi.org/10.1113/jphysiol.1992.sp019036

29. Higashida, H. (1988). Acetylcholine release by bradykinin, inositol 1,4,5-trisphosphate and phorbol dibutyrate in rodent neuroblastoma cells. *J. Physiol.*, 397(1), 209–222. https://doi.org/10.1113/jphysiol.1988.sp016996

30. Nelson, T. E. & Gruol, D. L. (2004). The chemokine CXCL10 modulates excitatory activity and intracellular calcium signaling in cultured hippocampal neurons. *J. Neuroimmunol.*, 156(1–2), 74–87. https://doi.org/10.1016/j.jneuroim.2004.07.009

31. Mahakunakorn, P. et al. (2003). Cytoprotective and cytotoxic effects of curcumin: Dual action on H_2O_2-induced oxidative cell damage in NG108-15 cells. *Biol. Pharm. Bull.*, 26(5), 725–728. https://doi.org/10.1248/bpb.26.725

32. Wong, D. Z. H., Kadir, H. A. & Ling, S. K. (2012). Bioassay-guided isolation of neuroprotective compounds from Loranthus parasiticus against H_2O_2-induced oxidative damage in NG108-15 cells. *J. Ethnopharmacol.*, 139(1), 256–264. https://doi.org/10.1016/j.jep.2011.11.010

33. Guimond, M. O., Roberge, C. & Gallo-Payet, N. (2010). Fyn is involved in angiotensin II type 2 receptor-induced neurite outgrowth, but not in p42/p44mapk in NG108-15 cells. *Mol. Cell. Neurosci.*, 45(3), 201–212. https://doi.org/10.1016/j.mcn.2010.06.011

34. Jin, E. & Sano, M. (2008). Neurite outgrowth of NG108-15 cells induced by heat shock protein 90 inhibitors. *Cell Biochem. Funct.*, 26(8), 825–832. https://doi.org/10.1002/cbf.1458

35.   Lozano, A. M., Schmidt, M. & Roach, A. (1995). A convenient in vitro assay for the inhibition of neurite outgrowth by adult mammalian CNS myelin using immortalised neuronal cells. *J. Neurosci. Meth.*, 63(1–2), 23–28. https://doi.org/10.1016/0165-0270(95)00081-X

36.   Tsuji, T. et al. (2011). Ect2, an ortholog of Drosophila's pebble, negatively regulates neurite outgrowth in neuroblastoma × glioma hybrid NG108-15 cells. *Cell. Mol. Neurobiol.*, 31(5), 663–668. https://doi.org/10.1007/s10571-011-9668-3